FLOMEKO2019
18th International Flow Measurement Conference
Portugal | Lisbon | LNEC | 26-28 june 2019

Comparison of calibrations of wind speed meters with a large blockage effect

J. Geršl[1], P. Busche[2], M. de Huu[3], D. Pachinger[4], H. Müller[5], K. Hölper[6], A. Bertašienė[7], M. Vilbaste[8], I. Care[9], H. Kaykısızlı[10], L. Maar[11], S. Haack[12]

[1]Czech Metrology Institute, Okruzni 31,63800 Brno, Czech Republic
[2]Deutsche WindGuard Wind Tunnel Services GmbH, Varel, Germany
[3]Federal Institute of Metrology METAS, Wabern, Switzerland
[4]BEV/E+E, Engerwitzdorf, Austria
[5]Physikalisch Technische Bundesanstalt, Braunschweig, Germany
[6]Westenberg Engineering, Köln, Germany
[7]Lithuanian Energy Institute, Kaunas, Lithuania
[8]Testing centre, University of Tartu, Tartu, Estonia
[9]CETIAT, Villeurbanne, France
[10]TÜBİTAK UME, Gebze / Kocaeli, Turkey
[11]Czech Hydrometeorological Institute, Prague, Czech Republic
[12]Danish Technological Institute, Aarhus, Denmark
E-mail (corresponding author): jgersl@cmi.cz

Abstract

In this paper we report on the first results of EURAMET project no. 1431 which was initiated in 2017 with a goal to experimentally determine systematic deviations of calibration results of vane and cup anemometers due to various boundary conditions in different wind tunnels especially in wind tunnels with open test section where theoretical models are missing. For that purpose 3 vane anemometers and 2 cup anemometers of various dimensions have been calibrated in 14 wind tunnels with various types and sizes of test sections ranging from 15 cm to 100 cm in diameter. This paper provides the first look to calibration data from the recently completed measurements. On top of that, velocity disturbance fields in front of the 5 tested anemometers have been measured in order to avoid mixing of the effect of boundary conditions with other source of deviations due to placing a reference meter to an area influenced by a meter under test. The velocity disturbance fields reported in this paper can be useful for all air speed calibration laboratories giving an idea how large these deviations can be and what is the optimal position and distance of a reference meter.

1. Introduction

When an anemometer is calibrated in a wind tunnel the velocity indication of the meter is influenced by flow conditions at a boundary of a test section of the wind tunnel leading to the so called blockage effect. The larger is the meter compared to the test section diameter the more significant the blockage effect is. The effect also depends on a type of the test section (open or closed) and on a type of the anemometer tested. Moreover, it is desirable to place a reference anemometer to a position where the velocity field is not significantly influenced by the meter under test which may not be possible for large meters leading to another source of systematic errors in anemometer calibrations [1, 2]. These effects were observed also in inter-laboratory comparisons of wind-speed calibration laboratories and in [3] it was concluded that the results of the comparisons indicate a need for more attention to blockage effects during air speed calibrations and their effect on air speed uncertainty statements.

To make the calibration results from various wind tunnels comparable they should be corrected to values corresponding to certain standardized boundary conditions – e.g. to free stream conditions assuming an infinite asymptotically homogeneous velocity field with reference velocity given by the velocity at infinity (far enough from the anemometer). Or at least the size of such correction should be estimated and included in the uncertainty budget.

A theory of velocity corrections of measurements in wind tunnels with closed measurement section to the free stream conditions was developed by Glauert [4] and further extended by Mikkelsen and Sørensen [5]. Their

theory for closed measuring sections is reviewed and extended to open measuring sections in [6] or in the monograph [7]. This theory is suitable for horizontal axis wind turbines (vane anemometers) and it contains some simplifying assumptions and therefore its experimental validation is necessary.

In standards the blockage effect is addressed e.g. in [8] where a relative uncertainty contribution of 1/4 of the blockage ratio for closed measuring sections and 1/16 of the blockage ratio for open measuring sections is recommended in case of cup anemometer calibrations with Pitot tube as a reference, the blockage ratio being the ratio of the area of the anemometer projected to a plane perpendicular to the flow and the cross sectional area of the test section of a wind tunnel. For closed measuring sections use of the Maskell theorem [9] is recommended. Otherwise we are not aware of quantitative recommendations for blockage corrections or uncertainties. To eliminate these uncertainties the standards [8, 10] recommend not to exceed the blockage ratio of 10 % for wind tunnels with an open test section and 5 % for wind tunnels with a closed test section. The standard [11] recommends not to exceed 5 % in general. Experimental investigation of influence of the blockage effect to cup anemometer calibrations can be found e.g. in [12].

In this paper we report on the first results of the EURAMET project no. 1431. The final goal of this project is to experimentally determine the blockage effect corrections for vane and cup anemometers especially in case of wind tunnels with open test section. Such wind tunnels are widely used by calibration laboratories but the known correction models mostly apply to wind tunnels with closed test section. Mathematical modelling of processes at a boundary of air stream in open test sections is challenging [6].

Three vane anemometers and two cup anemometers of various sizes have been calibrated in 12 laboratories providing 14 wind tunnels with test sections of various types and sizes in a time period from November 2017 to March 2019. To separate the effect of boundary conditions from the effect of placing the reference meter to an area influenced by the meter under test the velocity fields in front of the 5 anemometers have been measured in a wind tunnel of the pilot laboratory (CMI). The measurements have been finished recently and the data analysis is in progress. This paper provides a first look and discussion of the measured data.

In Sections 2 and 3 of this paper we present details of the 14 participating wind tunnels and of the 5 used transfer standards. In Section 4 we show maps of the measured velocity disturbance fields in front of the transfer standards together with positions of the reference meters in the participating wind tunnels and we discuss their impact to systematic deviations between the participants. In Section 5 we present calibration curves of the 5 anemometers in the 14 wind tunnels and in Section 6 we discuss the results, draw conclusions and plan a future work.

2. Participating wind tunnels

The laboratories participating in the EURAMET project no. 1431 are (order according to a time of calibration): Czech Metrology Institute (CZ), BEV/E+E (AT), Physikalisch Technische Bundesanstalt (DE), Deutsche WindGuard Wind Tunnel Services (DE), Westenberg Engineering (DE), Lithuanian Energy Institute (LT), Testing centre - University of Tartu (EST), CETIAT (FR), Federal Institute of Metrology METAS (CH), TÜBİTAK UME (TR), Czech Hydrometeorological Institute (CZ), Danish Technological Institute (DK) (see also Figure 1).

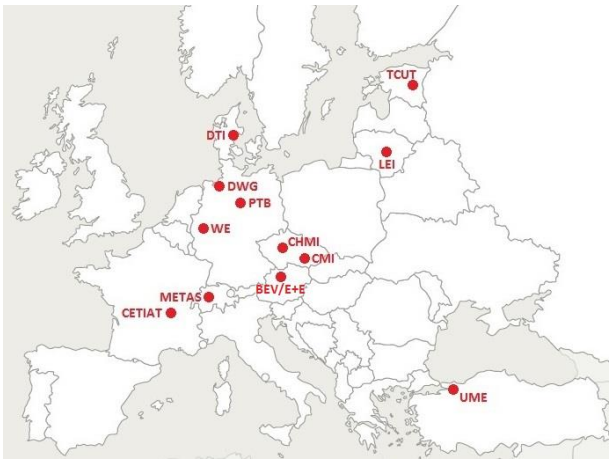

Figure 1: Map of the participating laboratories.

Table 1: Overview of the participating wind tunnels.

wind tunnel no.	wind tunnel type	test section type	nozzle shape	nozzle diameter /width (cm)
1	closed	open	square	100
2	open	box	circular	80
3	closed	open	rectang.	50 x 60
4	closed	open	circular	45
5	closed	box	circular	40
6	closed	open	circular	32
7	open	box	circular	31.5
8	closed	box	circular	25.5
9	closed	open	circular	25.5
10	open	box	circular	15.2
11	closed	closed	rectang.	74 x 49
12	closed	closed	square	51
13	open	closed	square	50
14	closed	closed	circular	40

An overview of parameters of the wind tunnels participating in the project is in Table 1. The wind tunnels are numbered according to the size of their test section from the largest to the smallest. First the wind tunnels with open test section or a test section bounded

by a box are listed (1-10) and then the wind tunnels with closed test section follow (11-14). By closed test section we mean a test section which is bounded by walls surrounding a space with the same cross-sectional area as the outlet nozzle of the wind tunnel, i.e. the walls are continuous prolongation of the nozzle. By a test section bounded by a box we mean a test section which is bounded by walls enclosing a space with a larger cross-sectional area than the area of the nozzle, i.e. the box is wider than the nozzle. This is a typical setup for open (Eiffel) type wind tunnels and there can be a large variety of dimensions of the box. By open test section we mean an unbounded test section. There can be other variants with slight deviations from the above definitions. E.g. the wind tunnel no. 1 has a wall (only) at the bottom and the wind tunnel no. 11 has three walls missing the bottom one.

3. Transfer standards

The following anemometers have been circulated among the participating laboratories:

1) Vane anemometer Schiltknecht MiniAir20 with the probe Macro; propeller diameter including frame 8.5 cm (Figure 2 top)
2) Vane anemometer Testo 0635 9340 with measuring unit Testo 445; propeller diameter including frame 10.7 cm (Figure 2 bottom)
3) Vane anemometer RM Young Gill Propeller MODEL 27106D/F; propeller diameter 20 cm; no frame (Figure 3)
4) Cup anemometer Vaisala WAA151; cup diameter 5.3 cm; propeller diameter 18.2 cm (Figure 4 right)
5) Cup anemometer Thies First Class Advanced type 4.3351.10.000; cup diameter 8 cm; propeller diameter 24 cm (Figure 4 left)

Figure 2: Anemometers Schiltknecht (top) and Testo (bottom).

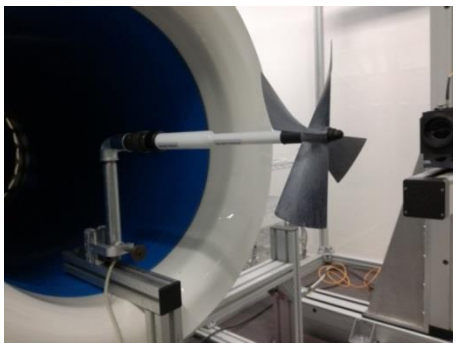

Figure 3: Anemometer RM Young Gill Propeller.

Figure 4: Anemometers Thies (left) and Vaisala (right).

The blockage ratio of an anemometer in a wind tunnel is determined as ratio of projected cross-sectional area of a cup wheel or propeller, sensor and support apparatus to the total area of a nozzle of the wind tunnel. The approximate blockage ratios of the 5 anemometers in the 14 wind tunnels are summarised in Table 2. Also wind tunnels exceeding the recommendations of [8, 10] on the blockage ratio, i.e. 10 % for open test sections and 5 % for closed test sections, are included in order to obtain more visible systematic deviations due to the blockage effect.

Table 2: Blockage ratios of the transfer standards.

wind tunnel	test sect.	vane Schilt.	vane Testo	vane RM Y.	cup Vais.	cup Thie.
		blockage ratio (%)				
1	open or box	0.57	0.90	1.3	1.4	2.2
2		1.1	1.8	2.5	2.8	4.4
3		1.9	3.0	4.2	4.7	7.4
4		3.6	5.7	7.9	8.9	13
5		4.5	7.2	10	9.8	16
6		7.1	11	x	11	22
7		7.3	12	16	12	23
8		11	18	25	18	35
9		11	18	x	x	x
10		31	50	x	x	x
11	closed	1.6	2.5	3.5	3.9	6.1
12		2.2	3.5	4.8	5.4	8.5
13		2.3	3.6	5.0	5.7	8.9
14		4.5	7.2	10	11	x

4. Velocity disturbance fields

In order to find the systematic deviations in calibration results due to boundary conditions in a test section of a wind tunnel it is necessary to have other sources of systematic deviations under control. One such possible source is the influence of a tested anemometer to the velocity field in a position where a reference anemometer is placed. Therefore, the velocity fields in front of the 5 tested anemometers have been measured in the wind tunnel of Czech Metrology Institute (CMI) for all velocities for which the calibrations have been performed (see Section 5) and maps of distribution of the reference meter positions of the participating laboratories have been created. The velocity fields in front of the anemometers may differ in different wind tunnels so the maps presented here, obtained in the wind tunnel of CMI, give just an estimate of a size of the effect of reference meter position.

The velocity fields have been measured with LDA placed on a 3D traversing system. Only the velocity component along the axis of the test section has been measured. The graphs presented here shows a velocity disturbance caused by the tested meter which is determined as a difference of the velocity field with the anemometer installed minus a velocity field measured in an empty test section. Since there can be a small unknown offset between the measurements with and without the anemometer the velocity disturbance fields are determined up to this offset and therefore the isolines in the plots are not provided with values. The step of the isolines is 0.2 % of a nominal velocity in all the plots Figure 5-11. This step is unaffected by the offset and therefore the plots show gradients of the velocity disturbance field and enable to determine velocity differences between the positions of the reference meters of the participants and also enable to determine an area in front of a meter where the influence of the meter is negligible by looking for a negligible gradients of the velocity disturbance field.

In Figures 5-7 the velocity disturbance fields in front of the vane anemometers are shown for the maximal velocities in which the anemometers have been calibrated (12 m/s for Testo and 20 m/s for Schiltknecht and RM Young). The fields were measured in a horizontal plane in a height of the centre of the anemometer's propeller in a grid of points with a step of 2 cm in both axial and transversal directions corresponding to the grid nodes in the plots. The flow direction in the plots is from bottom to the top (it is a top view of the horizontal plane), the bottom line being 2.5 cm behind the wind tunnel nozzle which is circular with a diameter of 45 cm. The width of the depicted area is 40 cm with axis of the test section in the middle, however, for the vane anemometers only a half of the plane was measured and the second half is mirrored assuming an axial symmetry of the meters and the flow. The tested anemometers are depicted as the grey blocks above the upper line. The projection of the anemometer shape is rectangular since this is a top view.

In Figures 8-11 the velocity disturbance fields in front of the cup anemometers are shown for the maximal velocity 20 m/s. The flow around the cup anemometers is not axially symmetric as in case of the vane anemometers and therefore it is not sufficient to measure the velocity field just in a horizontal half-plane. The Figures 8 and 10 again show the velocity disturbance field in a horizontal plane in a height of the centre of the anemometer's propeller with a difference that the whole plane was measured (no mirrored half-plane) and we can see the flow asymmetry in the measured field. The Figures 9 and 11 then show the velocity disturbance field in a vertical plane given by the axis of the wind tunnel test section and rotation axis of the anemometer. Only a half-plane above the propeller centre was measured since nobody place the reference meter below - in front of the anemometer body. In this case the flow direction is from left to right and again the left-most line of the grid is placed 2.5 cm behind the wind tunnel nozzle. The grid step is 2 cm as in all other plots.

The velocity disturbance fields for lower velocities, expressed in a relative way as percentage of a nominal velocity, look very similar to the ones for the maximal velocities depicted here. The fields for different velocities have been compared at the axis of the test section and slightly larger gradients have been observed only for the lowest velocity 0.5 m/s and for some of the meters (RM Young and Schiltknecht). Relative fluctuations of the velocity at the grid points are larger for lower velocities giving not so clear contours in the plots.

The positions of the reference anemometers of the particular laboratories are depicted as the red dots which are numbered according to the wind tunnel numbering introduced in the Table 1. The wind tunnel 5 is not included since the reference meter is placed 1.5 m in front of the meter under test. The wind tunnel 10 is not included since it uses a differential pressure measurement at the wind tunnel nozzle as a reference. The wind tunnel 14 is not included since the geometry data have not been submitted yet to the pilot laboratory. The reference meters of the wind tunnels 2 and 11 are placed 8 cm and 5 cm behind the right-most line of the plots. In case of the vane anemometers the positions of the reference meters which are not placed in the horizontal plane at the level of anemometer centre has been rotated and depicted in this plane taking the axial symmetry into account.

Discussion of the measured velocity disturbance fields is postponed to the Sections 5 and 6.

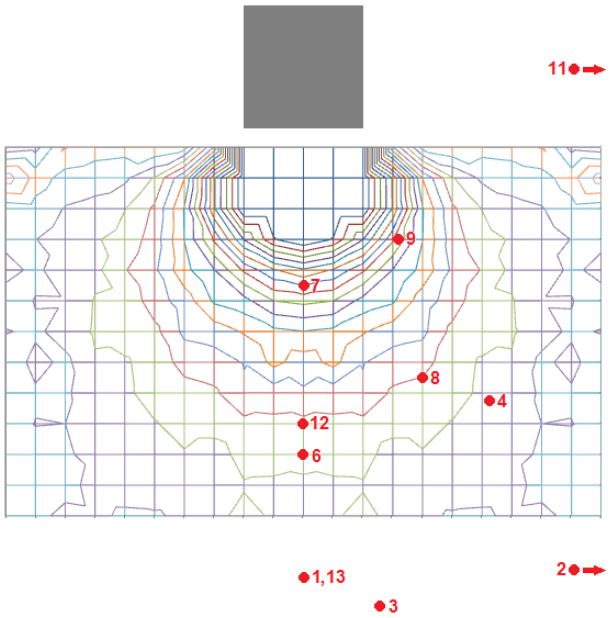

Figure 5: Velocity disturbance field, Schiltknecht, 20 m/s, isolines with step 0.2 % of 20 m/s (further explanation in the text).

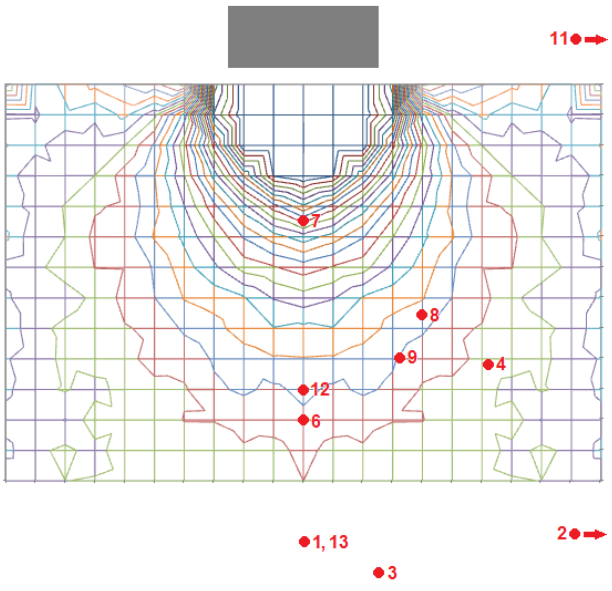

Figure 6: Velocity disturbance field, Testo, 12 m/s, isolines with step 0.2 % of 12 m/s (further explanation in the text).

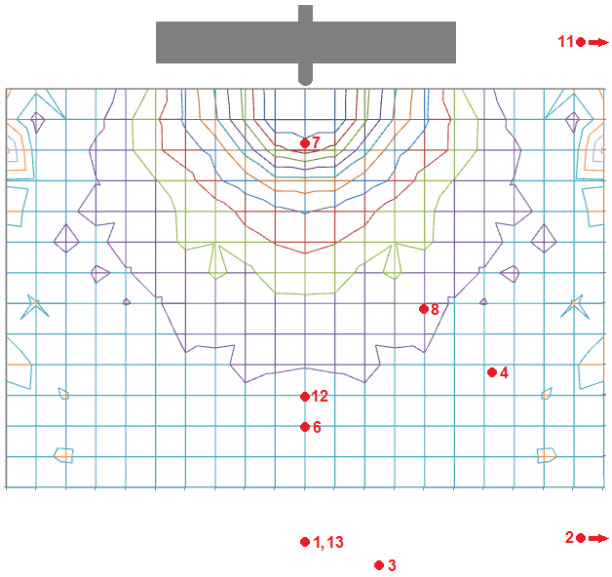

Figure 7: Velocity disturbance field, RM Young, 20 m/s, isolines with step 0.2 % of 20 m/s (further explanation in the text).

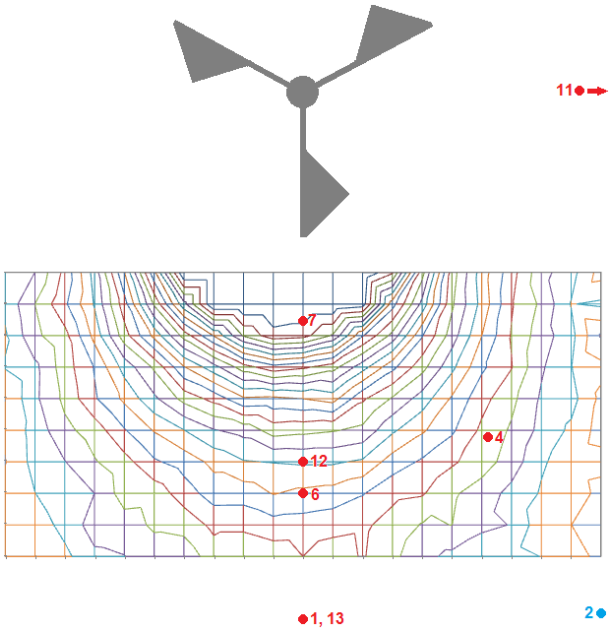

Figure 8: Velocity disturbance field in horizontal plane, Vaisala, 20 m/s, isolines with step 0.2 % of 20 m/s; the blue dot is 20 cm out of the plane towards the reader (further explanation in the text).

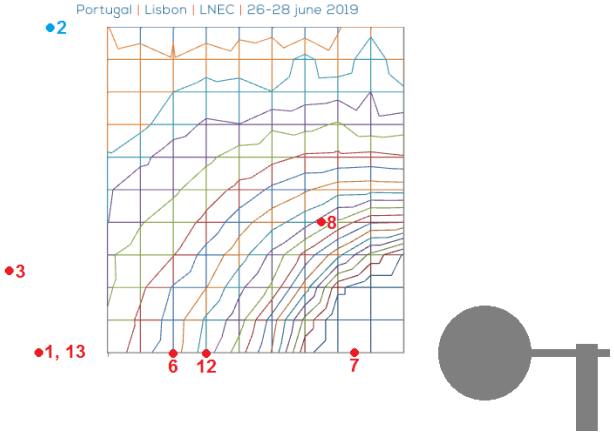

Figure 9: Velocity disturbance field in vertical plane, Vaisala, 20 m/s, isolines with step 0.2 % of 20 m/s; the blue dot is 20 cm out of the plane towards the reader (further explanation in the text).

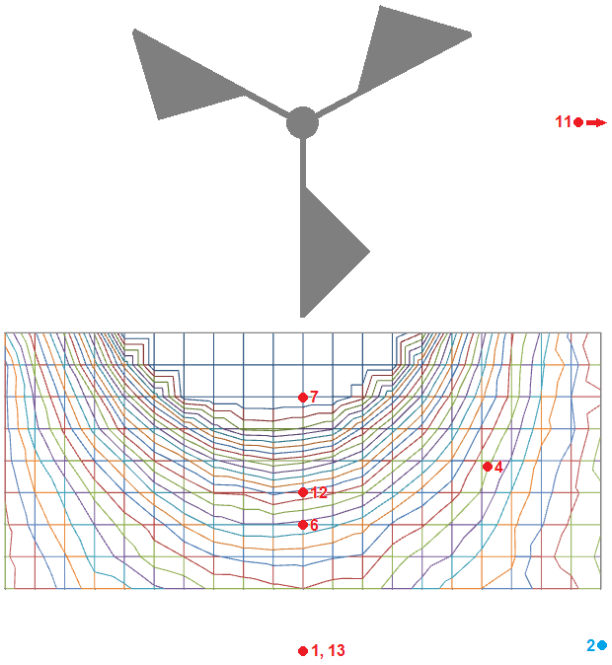

Figure 10: Velocity disturbance field in horizontal plane, Thies, 20 m/s, isolines with step 0.2 % of 20 m/s; the blue dot is 20 cm out of the plane towards the reader (further explanation in the text).

5. Calibration results

The anemometers Schiltknecht, RM Young and Thies have been calibrated in velocity points 0.5, 2, 5, 8, 12 and 20 m/s. In case of the anemometer Testo the 20 m/s was skipped since the meter has a range up to 15 m/s. For the anemometer Vaisala the 0.5 m/s was replaced by 1 m/s because of the starting treshold of the meter. The same mounting pipes have been used in all the laboratories. Each laboratory used its usual calibration procedure. During the measurement campaign (Nov 2017 – Mar 2019) all the meters have been calibrated

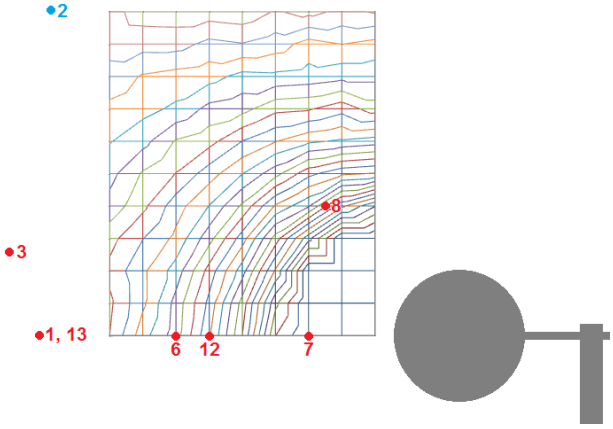

Figure 11: Velocity disturbance field in vertical plane, Thies, 20 m/s, isolines with step 0.2 % of 20 m/s; the blue dot is 20 cm out of the plane towards the reader (further explanation in the text).

6 times in the pilot lab (CMI) to evaluate the stability of the meters.

In Figures 12-16 the error curves of the 5 anemometers in the 14 wind tunnels are shown. The v_M axis displays a velocity indicated by a meter under test. The E axis displays the error of a meter, i.e. $E = v_M - v_{ref}$ with v_{ref} being a reference velocity. An error curve obtained in a particular wind tunnel has the number of the wind tunnel as defined in the Table 1. The curves drawn by a full line belong to wind tunnels satisfying the criteria of [8, 10] on the blockage ratio, i.e. less than 10 % for open test sections and less than 5 % for closed test sections. For test sections bounded by a box the 10 % criterion was used. The curves drawn by a dashed line belong to wind tunnels which exceed these limits. Uncertainty bars are not included for all the error curves in the Figures 12-16, however, for each velocity there is a pair of lines showing stability of the meter and typical expanded uncertainty of the calibrations. The span of the first line from a pair is given as difference between maximal and minimal error of the meter obtained during the six repeated calibrations in the pilot laboratory (CMI). The span of the second line from a pair is given as median of all expanded uncertainty intervals as reported by the participating laboratories. Only the span of the lines plays a role. The position of the lines in the plots has just a graphical justification.

In the Figure 12 with error curves of the smallest vane anemometer Schiltknecht we see a group of error curves at lower error values and then several curves above them. The shift of the wind tunnels 7and 9 to the larger error values can be explained by the close position of the reference meter (see Figure 5). The shift of 5, 13 and 14 is probably caused by a different kind of systematic error. The shift of 13 and 14 to the larger error values repeats also for the other meters.

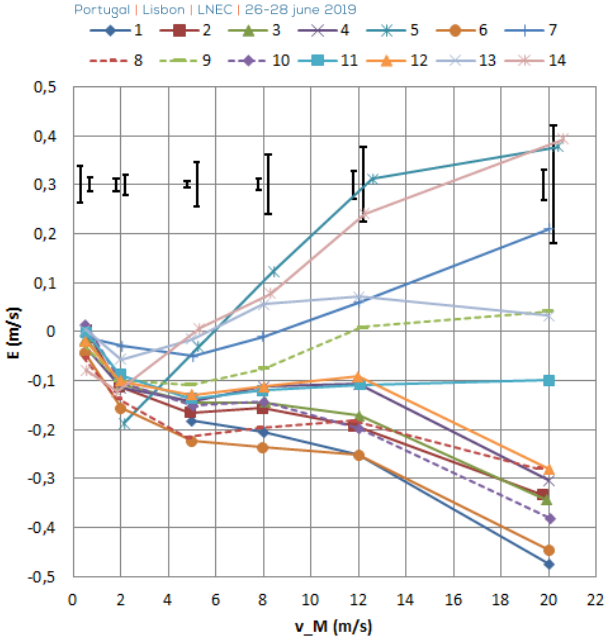

Figure 12: Error curves – vane anemometer Schiltknecht; for explanation of the graphical elements see the text.

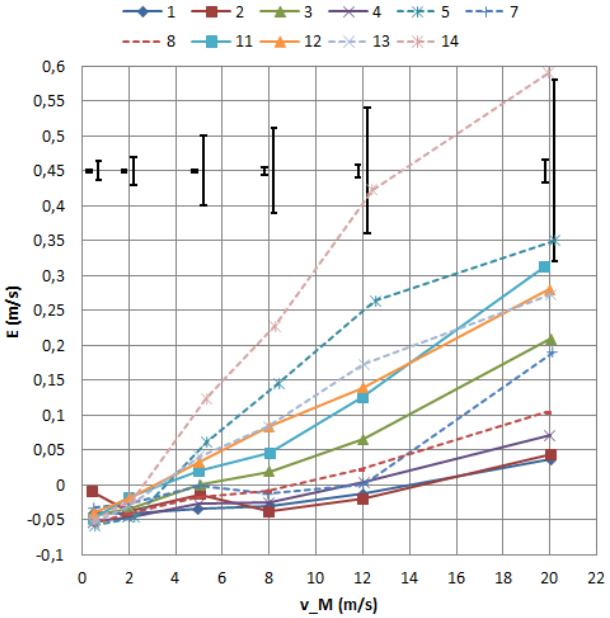

Figure 14: Error curves – vane anemometer RM Young; for explanation of the graphical elements see the text.

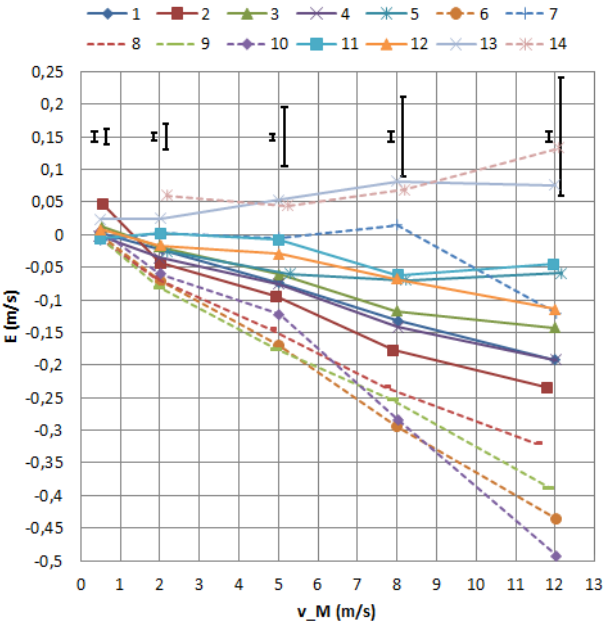

Figure 13: Error curves – vane anemometer Testo; for explanation of the graphical elements see the text.

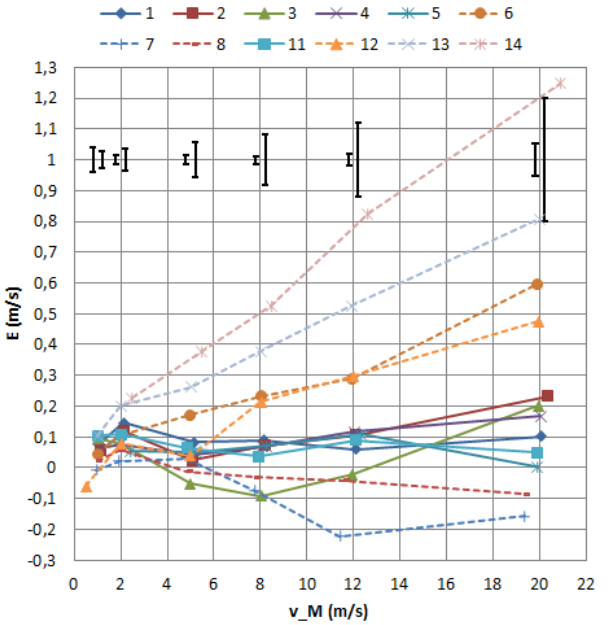

Figure 15: Error curves – cup anemometer Vaisala; for explanation of the graphical elements see the text.

In the Figure 13 with error curves of the midsize vane anemometer Testo we can see the error curves of the small wind tunnels (dashed lines) grouped at lower error values with exception of the wind tunnels 7 and 14 mentioned already above. The wind tunnel 9 in this case has the reference position shifted by 10 cm further from the MUT (see Figure 6) so the shift to the larger error values does not occur. The error curves of the larger wind tunnels (full lines) are grouped in the middle except no. 13 which is shifted similarly as for the Schiltknecht vane anemometer.

In the Figure 14 with error curves of the largest vane anemometer RM Young Gill Propeller we see quite good agreement between the error curves besides the curve 14 which is deviated also for the other meters. We

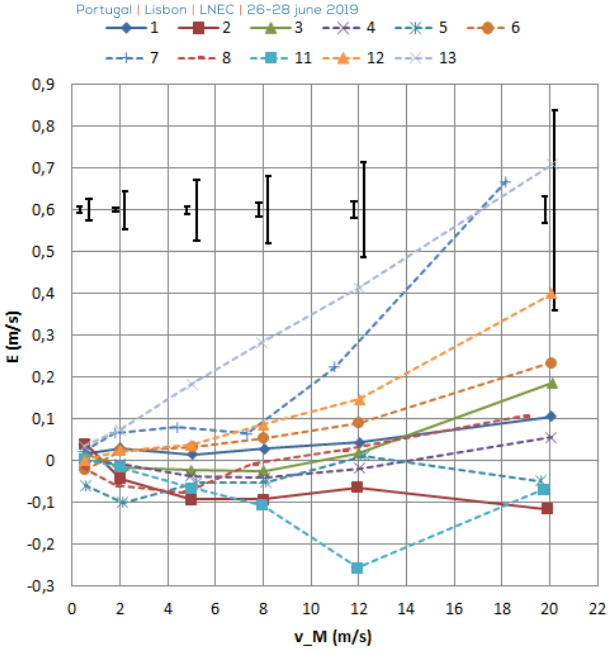

Figure 16: Error curves – cup anemometer Thies; for explanation of the graphical elements see the text.

cannot see a clear distinction between smaller wind tunnels (dashed lines) and larger wind tunnels (full lines). The reason could be that in spite of the large size of the meter the interaction with air stream is not so strong as follows from the Figure 7.

In the Figure 15 with error curves of the smaller cup anemometer Vaisala we can see a clear grouping of the curves belonging to the large wind tunnels (full lines) and the curves of the smaller wind tunnels (dashed lines) scattered around them. Similar behaviour can be seen also in the Figure 16 with the error curves of the larger cup anemometer Thies.

6. Discussion and conclusions

From the measured velocity disturbance fields (Figures 5-11) we see that the velocity gradients in front of the anemometers strongly depend not only on the anemometer size but also on the anemometer construction. The lowest influence was observed for the 20 cm vane anemometer RM Young Gill Propeller (see Figure 7) even if it has the blockage ratio which is the largest from the vane anemometers and comparable to the blockage ratio of the smaller cup anemometer Vaisala. The smaller vane anemometers Schiltknecht and Testo have a frame around their propellers which is not moving and stops the air causing the larger influence in front of the meters (see Figures 5 and 6). For the vane anemometers one can conclude that most of the wind tunnels have a reference meter in an area where the velocity gradient causes systematic deviations of a few tenths of percent between the labs which may be a significant value compared to typical uncertainty values, however, in most cases it is not a leading uncertainty component.

On the other hand for cup anemometers the velocity gradients in front of the meters are larger (see Figures 8-11). Even the largest wind tunnels in the project do not place their reference meter to a position with negligible velocity gradient and the systematic deviations between the labs due to the velocity gradient can exceed 1 % and therefore the velocity gradient becomes one of the dominant uncertainty sources.

Therefore, if we want to investigate the effect of boundary conditions in a wind tunnel and we want to avoid mixing with other effects like this effect of velocity gradient in front of a meter, it seems, that for the vane anemometers in this project it will be viable but for the cup anemometers it will be challenging.

Besides the velocity disturbance in front of the meters the calibration data (Figures 12-16) are influenced by various kinds of other systematic errors mixing with the effect of test section boundary conditions. Therefore, to achieve the goal of this project, also the other systematic deviations must be understood or compensated.

A compensation of additive errors not depending on a meter size could be realised by subtracting errors of two anemometers – one of them being small with a negligible blockage effect. For that purpose also a thermal anemometer Airflow TA440 was calibrated in all wind tunnels but because of its bad stability and other sources of systematic deviations (pressure setting, contamination) the data from this meter probably cannot be used for the compensation and we do not report the data from this meter here. Instead of the thermal anemometer additional measurements with a small vane anemometer with propeller diameter 22 mm have been planned.

We hope that further data analysis together with additional measurements will lead to visible trends in the anemometers' errors depending on a wind tunnel size.

Even if this project is not a classical inter-comparison and validation of uncertainty statements is not its primary purpose we can use the obtained data also for this.

In Table 3 a statistics of lab to lab equivalence degrees is shown. The equivalence degree between a lab 1 and a lab 2 is calculated as

$$En = \frac{|E_1 - E_2|}{\sqrt{U_1^2 + U_2^2 + D^2}} \qquad (1)$$

where E_1, E_2 are errors of the labs, U_1, U_2 are their expanded uncertainties and D is a contribution of instability of a meter given as the difference between maximal and minimal error obtained during the

6 repeated calibrations at CMI. The equivalence degrees have been calculated for all pairs of wind tunnels and the percentage of "successful" values not exceeding 1 is shown in the Table 3. The percentage is calculated for two wind tunnel sets – one set containing all the wind tunnels performing the calibration (rows denoted "all"), second containing only the wind tunnels satisfying the recommendation of [8, 10] on maximal blockage ratio (rows denoted "large"). In the column denoted "no. wts" an amount of the wind tunnels contained in the particular sets is shown.

Table 3: Statistics of lab to lab equivalence degrees ≤ 1. For explanation see the text.

		v (m/s)	0.5	2	5	8	12	20
meter	wt.set	no. wts	% En ≤ 1					
Sch.	all	14	99	64	53	49	47	49
	large	11	98	53	47	42	38	45
Tes.	all	14	88	58	51	51	47	
	large	8	81	93	75	71	68	
RM.	all	11	76	100	69	56	51	64
	large	6	73	100	93	80	87	80
Vai.	all	12	84	59	64	50	56	58
	large	6	87	67	80	73	93	93
Thi.	all	11	69	62	73	75	69	67
	large	3	67	67	67	67	100	67

For the meters Testo, RM Young and Vaisala we see that excluding the "small" wind tunnels significantly improves the percentage of En ≤ 1 which indicates underestimated uncertainties of the "small" wind tunnels. On the other hand the results of the smallest vane anemometer Schiltknecht show poor percentage of En ≤ 1 not depending on wind tunnel size indicating that significant part of the observed systematic deviations has an origin different than the blockage effect.

In any case the first look to the results of this project gives evidence that there is a work to be done in the uncertainty budgets for calibrations of vane and cup anemometers.

Acknowledgements

This work has been supported by technical development grants no. UTR 17601501, 18601501, 19601501 provided by the Czech Ministry of Industry and Trade.

References

[1] Care I and Arenas M, "On the impact of anemometer size on the velocity field in a closed wind tunnel", *Flow Measurement and Instrumentation*, **44**, 2-10, 2015.
[2] Sluše J, "Influence of blockage effect on measurement by vane anemometers", in *EPJ Web of Conferences*, **143**, 02110, 2017.
[3] Müller H, "Final report on EURAMET project No. 827: LDA-based intercomparison of anemometers", *Metrologia*, **50**, Technical Supplement, 2013.
[4] Glauert H, *Airplane Propellers, Aerodynamic Theory*, edited by Durand W F (New York, Dover), 1963, Chap. 7, Div. L
[5] Mikkelsen R and Sørensen J N, "Modelling of Wind Tunnel Blockage", in *Proceedings of the 2002 Global Windpower Conference and Exhibition* [CD-ROM], www.ewea.org.
[6] Sørensen J N, Shen W Z and Mikkelsen R, "Wall Correction Model for Wind Tunnels with Open Test Section", *AIAA Journal*, **44**, No. 8, August 2006.
[7] Sørensen J N, *General Momentum Theory for Horizontal Axis Wind Turbines* (Springer), 2016
[8] EN 61400-12-1: *Wind turbines – Part 12-1: Power performance measurements of electricity producing wind turbines, Annex F*, 2005.
[9] Maskell E C, "A Theory of the Blockage Effects on Bluff Bodies and Stalled Wings in a Closed Wind Tunnel", *Aeronautical Research Council Reports and Memoranda no.* 3400, 1963.
[10] ISO 17713-1: *Meteorology – Wind measurements – Part 1: Wind tunnel test methods for rotating anemometer performance*, 2007.
[11] ASTM D 5096-02: *Standard Test Method for Determining the Performance of a Cup Anemometer or Propeller Anemometer*, 2017.
[12] Westermann D, Balaresque N and Busche P, "Systematic deviation of the anemometer calibration due to geometrical interference", *Report of Deutsche WindGuard Wind Tunnel Services GmbH*, 2011.